J|A|C|S ARTICLES

Published on Web 10/29/2010

Biofunctionalization on Alkylated Silicon Substrate Surfaces via "Click" Chemistry

Guoting Qin,[†] Catherine Santos,[†] Wen Zhang,[†] Yan Li,[†] Amit Kumar,[†] Uriel J. Erasquin,[†] Kai Liu,[†] Pavel Muradov,[†] Barbara Wells Trautner,[‡] and Chengzhi Cai*,[†]

Department of Chemistry, University of Houston, Houston, Texas 77204, United States, and Department of Medicine, Infectious Diseases Section, Baylor College of Medicine, Houston, Texas 77030, United States

Received March 27, 2010; E-mail: cai@uh.edu

Abstract: Biofunctionalization of silicon substrates is important to the development of silicon-based biosensors and devices. Compared to conventional organosiloxane films on silicon oxide intermediate layers, organic monolayers directly bound to the nonoxidized silicon substrates via Si−C bonds enhance the sensitivity of detection and the stability against hydrolytic cleavage. Such monolayers presenting a high density of terminal alkynyl groups for bioconjugation via copper-catalyzed azide−alkyne 1,3-dipolar cycloaddition (CuAAC, a "click" reaction) were reported. However, yields of the CuAAC reactions on these monolayer platforms were low. Also, the nonspecific adsorption of proteins on the resultant surfaces remained a major obstacle for many potential biological applications. Herein, we report a new type of "clickable" monolayers grown by selective, photoactivated surface hydrosilylation of α,ω-alkenynes, where the alkynyl terminal is protected with a trimethylgermanyl (TMG) group, on hydrogen-terminated silicon substrates. The TMG groups on the film are readily removed in aqueous solutions in the presence of Cu(I). Significantly, the degermanylation and the subsequent CuAAC reaction with various azides could be combined into a single step in good yields. Thus, oligo(ethylene glycol) (OEG) with an azido tag was attached to the TMG−alkyne surfaces, leading to OEG-terminated surfaces that reduced the nonspecific adsorption of protein (fibrinogen) by >98%. The CuAAC reaction could be performed in microarray format to generate arrays of mannose and biotin with varied densities on the protein-resistant OEG background. We also demonstrated that the monolayer platform could be functionalized with mannose for highly specific capturing of living targets (*Escherichia coli* expressing fimbriae) onto the silicon substrates.

Introduction

Modification of silicon substrates with ultrathin organic films to allow for specific interactions with biological targets is important for the development of silicon-based bioelectrical sensors and devices,[1,2] nanoparticle probes,[3,4] nanowire sensors,[5] photonic devices,[6,7] cantilever sensors,[8,9] microarrays,[10,11] microfluidic,[12] and silicon−neuron interfaces.[2,13] These silicon-based transducers interconvert specific biomolecular interactions with electrical, mechanical, or optical signals of the silicon devices. Ideal thin film platforms on silicon substrates should allow specific binding of biological targets. To block nonspecific

[†] University of Houston.

[‡] Baylor College of Medicine.

(1) Hamers, R. J. *Annu. Rev. Anal. Chem.* **2008**, *1*, 707–736. Ciampi, S.; Gooding, J. J. *Chem.—Eur. J.* **2010**, *16*, 5961–5968. Yang, W. S.; Butler, J. E.; Russell, J. N.; Hamers, R. J. *Analyst* **2007**, *132*, 296–306. Shalek, A. K.; Robinson, J. T.; Karp, E. S.; Lee, J. S.; Ahn, D. R.; Yoon, M. H.; Sutton, A.; Jorgolli, M.; Gertner, R. S.; Gujral, T. S.; MacBeath, G.; Yang, E. G.; Park, H. *Proc. Natl. Acad. Sci. U. S. A.* **2010**, *107*, 1870–1875. Ainslie, K. M.; Desai, T. A. *Lab Chip* **2008**, *8*, 1864–1878. Vilan, A.; Yaffe, O.; Biller, A.; Salomon, A.; Kahn, A.; Cohen, D. *Adv. Mater.* **2010**, *22*, 140–159. Touahir, L.; Moraillon, A.; Allongue, P.; Chazalviel, J. N.; de Villeneuve, C. H.; Ozanam, F.; Solomon, I.; Gouget-Laemmel, A. C. *Biosens. Bioelectron.* **2009**, *25*, 952–955.

(2) Hochberg, L. R.; Serruya, M. D.; Friehs, G. M.; Mukand, J. A.; Saleh, M.; Caplan, A. H.; Branner, A.; Chen, D.; Penn, R. D.; Donoghue, J. P. *Nature* **2006**, *442*, 164–171.

(3) He, Y.; Kang, Z. H.; Li, Q. S.; Tsang, C. H. A.; Fan, C. H.; Lee, S. T. *Angew. Chem.,Int. Ed.* **2009**, *48*, 128–132. He, Y.; Su, Y. Y.; Yang, X. B.; Kang, Z. H.; Xu, T. T.; Zhang, R. Q.; Fan, C. H.; Lee, S. T. *J. Am. Chem. Soc.* **2009**, *131*, 4434–4438. Shiohara, A.; Hanada, S.; Prabakar, S.; Fujioka, K.; Lim, T. H.; Yamamoto, K.; Northcote, P. T.; Tilley, R. D. *J. Am. Chem. Soc.* **2010**, *132*, 248–253. Erogbogbo, F.; Yong, K. T.; Roy, I.; Xu, G. X.; Prasad, P. N.; Swihart, M. T. *ACS Nano* **2008**, *2*, 873–878. Okamoto, H.; Kumai, Y.; Sugiyama, Y.; Mitsuoka, T.; Nakanishi, K.; Ohta, T.; Nozaki, H.; Yamaguchi, S.; Shirai, S.; Nakano, H. *J. Am. Chem. Soc.* **2010**, *132*, 2710–2718. Orosco, M. M.; Pacholski, C.; Miskelly, G. M.; Sailor, M. J. *Adv. Mater.* **2006**, *18*, 1393–1396. Tilley, R. D.; Yamamoto, K. *Adv. Mater.* **2006**, *18*, 2053–2056.

(4) Rosso-Vasic, M.; Spruijt, E.; Popovic, Z.; Overgaag, K.; van Lagen, B.; Grandidier, B.; Vanmaekelbergh, D.; Dominguez-Gutierrez, D.; De Cola, L.; Zuilhof, H. *J. Mater. Chem.* **2009**, *19*, 5926–5933.

(5) Gao, X. P. A.; Zheng, G. F.; Lieber, C. M. *Nano Lett.* **2010**, *10*, 547–552. Ben Ishai, M.; Patolsky, F. *J. Am. Chem. Soc.* **2009**, *131*, 3679–3689. Bunimovich, Y. L.; Shin, Y. S.; Yeo, W. S.; Amori, M.; Kwong, G.; Heath, J. R. *J. Am. Chem. Soc.* **2006**, *128*, 16323–16331. Cohen-Karni, T.; Timko, B. P.; Weiss, L. E.; Lieber, C. M. *Proc. Natl. Acad. Sci. U.S.A.* **2009**, *106*, 7309–7313. Martinez, J. A.; Misra, N.; Wang, Y. M.; Stroeve, P.; Grigoropoulos, C. P.; Noy, A. *Nano Lett.* **2009**, *9*, 1121–1126. Patolsky, F.; Zheng, G.; Lieber, C. M. *Nanomedicine* **2006**, *1*, 51–65. Wang, W. U.; Chen, C.; Lin, K. H.; Fang, Y.; Lieber, C. M. *Proc. Natl. Acad. Sci. U.S.A.* **2005**, *102*, 3208–3212.

10.1021/ja1025497

binding, the silicon substrates are commonly modified with organosiloxane films presenting oligo- or poly(ethylene glycol) (OEG or PEG) on the oxide surface of the substrates.[14] However, the protein resistance and stability of these films are not satisfactory, probably due to the relatively low packing density of the films and the high density of defects resulting from the interaction of silanols with the hydrophilic OEG chains.[14,15] We and others have developed monolayers presenting OEG, which are directly bound on nonoxidized silicon substrates via Si−C bonds.[7,9,16−19] Formation of the Si−C bonds is via surface hydrosilylation on hydrogen-terminated silicon surfaces[20−22] using OEG-terminated alkenes, such as **1** in Scheme 1.[9,17−19,23] Our OEG-terminated monolayers are highly protein resistant and stable in phosphate-buffered saline (PBS).[19]

Herein, we describe the development of a monolayer platform presenting OEG−alkyne on silicon substrates that allows efficient bioconjugation using copper-catalyzed azide−alkyne 1,3-dipolar cycloaddition (CuAAC, a "click" reaction).[24−26]

Among a variety of reactions for biofunctionalization on surfaces,[10,27] CuAAC reaction is specific and bioorthogonal and can be performed under physiological conditions.[25,26,28] It has been used on a wide variety of substrates.[4,29−32] To use CuAAC reaction on alkylated silicon substrates, we need to incorporate either azido or alkynyl groups on the surface. Azido-presenting monolayers on silicon were prepared from H−Si surfaces through two steps: chlorination[33] or hydrosilylation with Br-terminated alkenes[34] followed by substitution with NaN_3. Direct attachment of N_3-alkenes onto H−Si surfaces by hydrosilylation has not been reported and failed in our attempts, likely because the azido groups readily decompose during photo or thermally activated hydrosilylation via a highly reactive nitrenen intermediate.[35]

Alternative to azido-presenting monolayers, two types of alkynyl-presenting monolayers bound on silicon via Si−C bonds were reported.[30,32,36,37] The first type was prepared by ethynyl-

(6) Alvarez, S. D.; Derfus, A. M.; Schwartz, M. P.; Bhatia, S. N.; Sailor, M. J. *Biomaterials* **2009**, *30*, 26–34. Sailor, M. J.; Wu, E. C. *Adv. Funct. Mater.* **2009**, *19*, 3195–3208. Qu, Y. Q.; Liao, L.; Li, Y. J.; Zhang, H.; Huang, Y.; Duan, X. F. *Nano Lett.* **2009**, *9*, 4539–4543. Ouyang, H.; Christophersen, M.; Viard, R.; Miller, B. L.; Fauchet, P. M. *Adv. Funct. Mater.* **2005**, *15*, 1851–1859.

(7) Kilian, K. A.; Bocking, T.; Gaus, K.; Gal, M.; Gooding, J. J. *Biomaterials* **2007**, *28*, 3055–3062. Kilian, K. A.; Bocking, T.; Ilyas, S.; Gaus, K.; Jessup, W.; Gal, M.; Gooding, J. J. *Adv. Funct. Mater.* **2007**, *17*, 2884–2890. Kilian, K. A.; Boecking, T.; Gooding, J. J. *Chem. Commun.* **2009**, 630–640.

(8) Ilic, B.; Yang, Y.; Craighead, H. G. *Appl. Phys. Lett.* **2004**, *85*, 2604–2606. Singamaneni, S.; LeMieux, M. C.; Lang, H. P.; Gerber, C.; Lam, Y.; Zauscher, S.; Datskos, P. G.; Lavrik, N. V.; Jiang, H.; Naik, R. R.; Bunning, T. J.; Tsukruk, V. V. *Adv. Mater.* **2008**, *20*, 653–680.

(9) Yam, C. M.; Xiao, Z. D.; Gu, J. H.; Boutet, S.; Cai, C. Z. *J. Am. Chem. Soc.* **2003**, *125*, 7498–7499. Gu, J. H.; Xiao, Z. D.; Yam, C. M.; Qin, G. T.; Deluge, M.; Boutet, S.; Cai, C. Z. *Biophys. J.* **2005**, *89*, L31–L33.

(10) Jonkheijm, P.; Weinrich, D.; Schroder, H.; Niemeyer, C. M.; Waldmann, H. *Angew. Chem., Int. Ed.* **2008**, *47*, 9618–9647.

(11) Cha, T.; Guo, A.; Jun, Y.; Pei, D. Q.; Zhu, X. Y. *Proteomics* **2004**, *4*, 1965–1976. Nijdam, A. J.; Cheng, M. M. C.; Geho, D. H.; Fedele, R.; Herrmann, P.; Killian, K.; Espina, V.; Petricoin, E. F.; Liotta, L. A.; Ferrari, M. *Biomaterials* **2007**, *28*, 550–558.

(12) Domachuk, P.; Tsioris, K.; Omenetto, F. G.; Kaplan, D. L. *Adv. Mater.* **2010**, *22*, 249–260. Stern, E.; Vacic, A.; Rajan, N. K.; Criscione, J. M.; Park, J.; Ilic, B. R.; Mooney, D. J.; Reed, M. A.; Fahmy, T. M. *Nat. Nanotechnol.* **2010**, *5*, 138–142.

(13) Fromherz, P. *Solid-State Electron.* **2008**, *52*, 1364–1373.

(14) Jo, S.; Park, K. *Biomaterials* **2000**, *21*, 605–616. Lee, S. W.; Laibinis, P. E. *Biomaterials* **1998**, *19*, 1669–1675.

(15) Dekeyser, C. M.; Buron, C. C.; Mc Evoy, K.; Dupont-Gillain, C. C.; Marchand-Brynaert, J.; Jonas, A. M.; Rouxhet, P. G. *J. Colloid Interface Sci.* **2008**, *324*, 118–126. Harbers, G. M.; Emoto, K.; Greef, C.; Metzger, S. W.; Woodward, H. N.; Mascali, J. J.; Grainger, D. W.; Lochhead, M. J. *Chem. Mater.* **2007**, *19*, 4405–4414. Hoffmann, C.; Tovar, G. E. M. *J. Colloid Interface Sci.* **2006**, *295*, 427–435. Tsukagoshi, T.; Kondo, Y.; Yoshino, N. *Colloid Surf. B: Biointerfaces* **2007**, *54*, 82–87.

(16) Lasseter, T. L.; Cai, W.; Hamers, R. J. *Analyst* **2004**, *129*, 3–8. Wang, C.; Landis, E. C.; Franking, R.; Hamers, R. J. *Acc. Chem. Res.* **2010**, *43*, 1205–1215. Clare, T. L.; Clare, B. H.; Nichols, B. M.; Abbott, N. L.; Hamers, R. J. *Langmuir* **2005**, *21*, 6344–6355. Bocking, T.; Kilian, K. A.; Hanley, T.; Ilyas, S.; Gaus, K.; Gal, M.; Gooding, J. J. *Langmuir* **2005**, *21*, 10522–10529. Bocking, T.; Killan, K. A.; Gaus, K.; Gooding, J. J. *Langmuir* **2006**, *22*, 3494–3496. Yu, Q. K.; Qin, G. T.; Darne, C.; Cai, C. Z.; Wosik, W.; Pei, S. S. *Sens. Actuators A: Phys.* **2006**, *126*, 369–374.

(17) Yam, C. M.; Lopez-Romero, J. M.; Gu, J. H.; Cai, C. Z. *Chem. Commun.* **2004**, 2510–2511. Yam, C. M.; Gu, J. H.; Li, S.; Cai, C. Z. *J. Colloid Interface Sci.* **2005**, *285*, 711–718.

(18) Gu, J. H.; Yam, C. M.; Li, S.; Cai, C. Z. *J. Am. Chem. Soc.* **2004**, *126*, 8098–8099.

(19) Qin, G. T.; Cai, C. Z. *Chem. Commun.* **2009**, 5112–5114.

(20) Linford, M. R.; Fenter, P.; Eisenberger, P. M.; Chidsey, C. E. D. *J. Am. Chem. Soc.* **1995**, *117*, 3145–3155. Buriak, J. M. *Chem. Rev.* **2002**, *102*, 1271–1308.

(21) Cicero, R. L.; Linford, M. R.; Chidsey, C. E. D. *Langmuir* **2000**, *16*, 5688–5695.

(22) Ciampi, S.; Harper, J. B.; Gooding, J. J. *Chem. Soc. Rev.* **2010**, *39*, 2158–2183.

(23) Qin, G. T.; Zhang, R.; Makarenko, B.; Kumar, A.; Rabalais, W.; Romero, J. M. L.; Rico, R.; Cai, C. Z. *Chem. Commun.* **2010**, *46*, 3289–3291.

(24) Rostovtsev, V. V.; Green, L. G.; Fokin, V. V.; Sharpless, K. B. *Angew. Chem., Int. Ed.* **2002**, *41*, 2596–2599. Hein, J. E.; Fokin, V. V. *Chem. Soc. Rev.* **2010**, *39*, 1302–1315.

(25) Meldal, M.; Tornoe, C. W. *Chem. Rev.* **2008**, *108*, 2952–3015.

(26) Hong, V.; Presolski, S. I.; Ma, C.; Finn, M. G. *Angew. Chem., Int. Ed.* **2009**, *48*, 9879–9883.

(27) Wong, L. S.; Khan, F.; Micklefield, J. *Chem. Rev.* **2009**, *109*, 4025–4053.

(28) Hudalla, G. A.; Murphy, W. L. *Langmuir* **2009**, *25*, 5737–5746. Le Droumaguet, C.; Wang, C.; Wang, Q. *Chem. Soc. Rev.* **2010**, *39*, 1233–1239.

(29) Bryan, M. C.; Fazio, F.; Lee, H. K.; Huang, C. Y.; Chang, A.; Best, M. D.; Calarese, D. A.; Blixt, C.; Paulson, J. C.; Burton, D.; Wilson, I. A.; Wong, C. H. *J. Am. Chem. Soc.* **2004**, *126*, 8640–8641. Lutz, J. F. *Angew. Chem., Int. Ed.* **2007**, *46*, 1018–1025. Nandivada, H.; Jiang, X. W.; Lahann, J. *Adv. Mater.* **2007**, *19*, 2197–2208. Nebhani, L.; Barner-Kowollik, C. *Adv. Mater.* **2009**, *21*, 3442–3468. Collman, J. P.; Devaraj, N. K.; Chidsey, C. E. D. *Langmuir* **2004**, *20*, 1051–1053. Gallant, N. D.; Lavery, K. A.; Amis, E. J.; Becker, M. L. *Adv. Mater.* **2007**, *19*, 965–969. Fleming, D. A.; Thode, C. J.; Williams, M. E. *Chem. Mater.* **2006**, *18*, 2327–2334. Li, H. M.; Cheng, F. O.; Duft, A. M.; Adronov, A. *J. Am. Chem. Soc.* **2005**, *127*, 14518–14524. O'Reilly, R. K.; Joralemon, M. J.; Wooley, K. L.; Hawker, C. J. *Chem. Mater.* **2005**, *17*, 5976–5988. Prakash, S.; Long, T. M.; Selby, J. C.; Moore, J. S.; Shannon, M. A. *Anal. Chem.* **2007**, *79*, 1661–1667. White, M. A.; Johnson, J. A.; Koberstein, J. T.; Turro, N. J. *J. Am. Chem. Soc.* **2006**, *128*, 11356–11357. Zhang, Y.; Luo, S. Z.; Tang, Y. J.; Yu, L.; Hou, K. Y.; Cheng, J. P.; Zeng, X. Q.; Wang, P. G. *Anal. Chem.* **2006**, *78*, 2001–2008. Devadoss, A.; Chidsey, C. E. D. *J. Am. Chem. Soc.* **2007**, *129*, 5370–5371. Duckworth, B. P.; Xu, J. H.; Taton, T. A.; Guo, A.; Distefano, M. D. *Bioconjugate Chem.* **2006**, *17*, 967–974. Sun, X. L.; Stabler, C. L.; Cazalis, C. S.; Chaikof, E. L. *Bioconjugate Chem.* **2006**, *17*, 52–57. Santos, C. M.; Kumar, A.; Zhang, W.; Cai, C. Z. *Chem. Commun.* **2009**, 2854–2856. Kumar, A.; Erasquin, U. J.; Qin, G.; Li, K.; Cai, C. Z. *Chem. Commun.* **2010**, *46*, 5746–5748.

(30) Ciampi, S.; Bocking, T.; Kilian, K. A.; James, M.; Harper, J. B.; Gooding, J. J. *Langmuir* **2007**, *23*, 9320–9329.

(31) Lin, P. C.; Ueng, S. H.; Tseng, M. C.; Ko, J. L.; Huang, K. T.; Yu, S. C.; Adak, A. K.; Chen, Y. J.; Lin, C. C. *Angew. Chem., Int. Ed.* **2006**, *45*, 4286–4290.

(32) Rohde, R. D.; Agnew, H. D.; Yeo, W. S.; Bailey, R. C.; Heath, J. R. *J. Am. Chem. Soc.* **2006**, *128*, 9518–9525.

(33) Cao, P. G.; Xu, K.; Heath, J. R. *J. Am. Chem. Soc.* **2008**, *130*, 14910–14911.

(34) Haensch, C.; Hoeppener, S.; Schubert, U. S. *Nanotechnology* **2008**, 19. Giacomo, M. A.; Fabrizio, C.; Franco, D.; Robertino, Z.; Maurizio, C.; Francesca, I. M. *J. Nanosci. Nanotechnol.* **2010**, *10*, 2901–2907.

(35) Scriven, E. F. V. *Azides and nitrenes: reactivity and utility*; Academic Press: Orlando, FL, 1984.

Scheme 1. Preparation of the TMG-Terminated Film (**A**) from the Alkenyne **2** and Its Deprotection to the Ethynyl-Presenting Film **B** and Direct CuAAC Reactions with the Azides **3**−**7** Promoted by Cu^+ and the Ligand **10** To Form Films Presenting CF_3 (**C**), OEG (**D**), Mannose (**E**), Glucose (**F**), and Biotin (**G**)

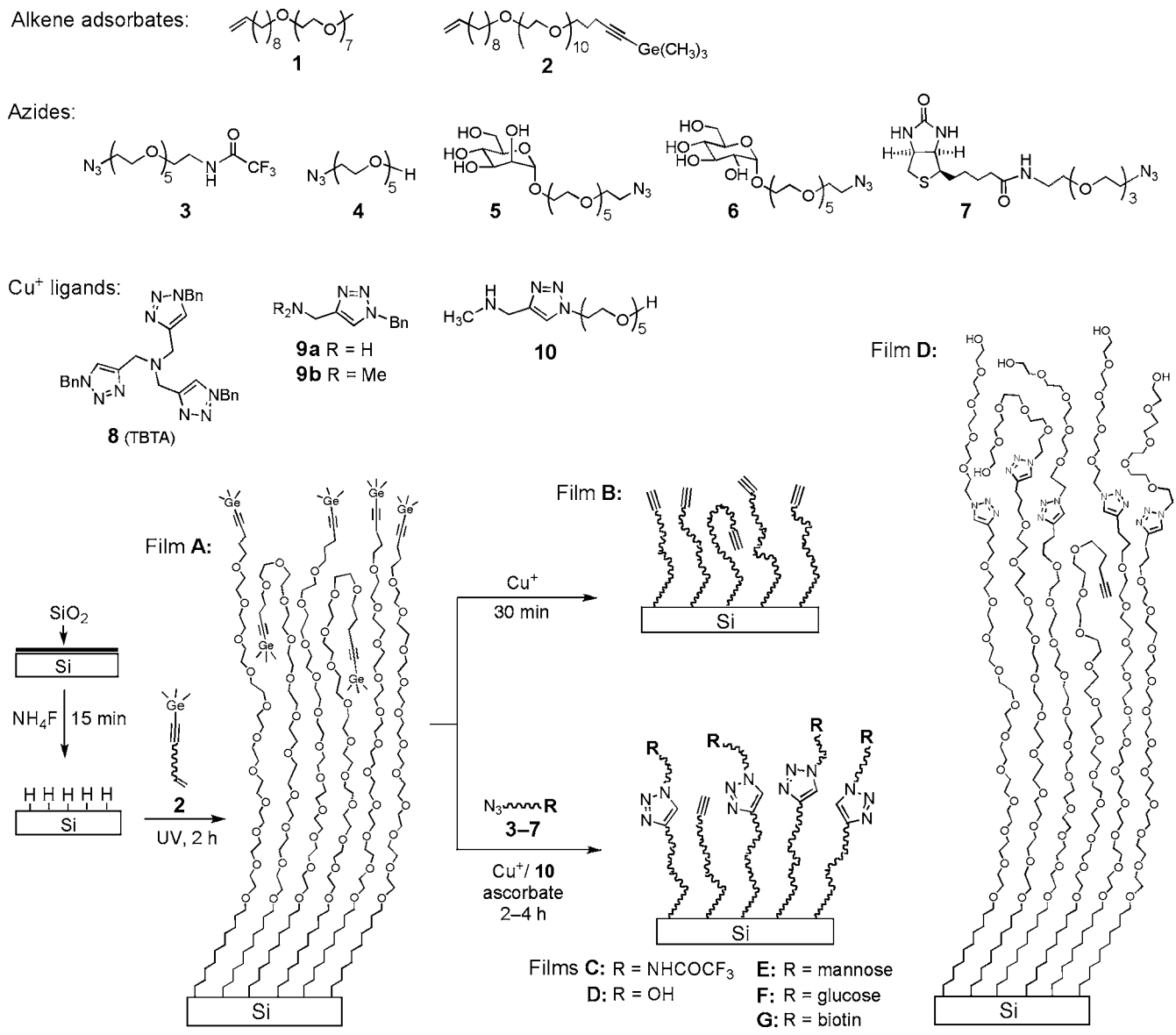

ation of chlorinated Si(111) surfaces, providing a nearly complete coverage of ethynyl groups directly bound to the silicon substrate. The close packing of the rigid ethynyl groups on the atomically flat surface likely prevented the CuAAC reaction; the reaction could only occur at the step edges and defect sites, leading to a low overall yield (7%).[32,36] The second type was prepared by Gooding and co-workers elegantly from a commercially available distal diyne (1,8-nonadiyne) by thermally activated hydrosilylation.[30,37] The subsequent grafting of an OEG−azide to the monolayer via CuAAC reaction proceeded with a modest yield (42%−51%). Unfortunately, the protein resistance of the resultant OEG-terminated films was not satisfactory (adsorbing ~25% monolayer of bovine serum albumin), likely due to the low density of the OEG chains grafted on the hydrophobic alkynyl surface.[30] The reasons for the lower yields of the CuAAC reactions on alkynyl vs azido surfaces were unclear and could be due to steric hindrance, side reactions, and/or polymerization of the well-ordered alkynes.[25] Gooding and co-workers showed that decreasing the density of the alkynyl chains by codeposition with alkyl chains increased the yields of the subsequent CuAAC reaction up to 90%, attributed to the decrease of the above factors.[37] However, this approach might not provide sufficient density of OEG chains for resisting nonspecific adsorption of proteins.

Herein we report a versatile "clickable" monolayer platform that addresses the above issues. This platform is easily grown by photoactivated hydrosilylation of an enyne, where the alkynyl terminal is masked with a trimethylgermanyl (TMG) group, on hydrogen-terminated silicon surfaces. The removal of the TMG group and the subsequent CuAAC reaction can be performed in a single step in good yields. Significantly, nonspecific adsorption of proteins on the resultant OEG surfaces was reduced by >98%, attributable to the unique alkynyl−OEG−alkyl platform and the efficient grafting of the OEG chains onto the

(36) Hurley, P. T.; Nemanick, E. J.; Brunschwig, B. S.; Lewis, N. S. *J. Am. Chem. Soc.* **2006**, *128*, 9990–9991.
(37) Ciampi, S.; Eggers, P. K.; Le Saux, G.; James, M.; Harper, J. B.; Gooding, J. J. *Langmuir* **2009**, *25*, 2530–2539.

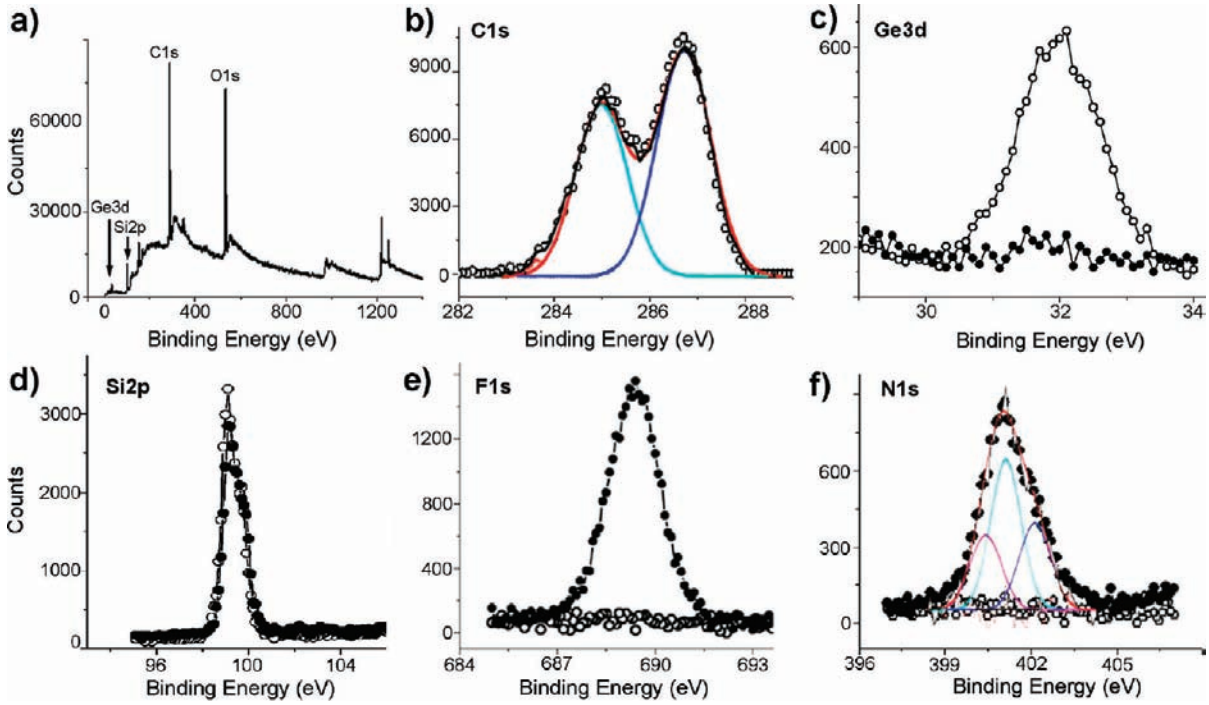

Figure 1. Selected XPS data obtained on films **A** before and after degermanylation and CuAAC reactions. XPS survey (a) and narrow scan for C1s (b, with deconvolution) of films **A**, and narrow scans for Ge3d (c), Si2p (d), F1s (e), and N1s (f, with deconvolution) before (empty circle) and after (solid dot) CuAAC reaction with the CF_3-terminated azide **3**.

platform. The reaction could be performed in microarray format to attach azido-labeled molecules (e.g., mannose and biotin) with varied densities on an OEG background to allow specific binding of targeted molecules. We also demonstrate that the monolayer platforms could be functionalized with mannose to specifically capture living targets (*E. coli* expressing mannose-binding fimbria) onto the silicon substrates.

Results and Discussion

Monolayer Preparation and Deprotection. Our approach to preparation of alkynyl-presenting ("clickable") monolayers on silicon substrates is based on the selective hydrosilylation of α,ω-alkenynes on H−Si surfaces. In this approach, the terminal alkynyl group needs to be masked with a bulky protecting group since it is usually more reactive than the alkene group.[38] The most common protecting groups for terminal alkynes are trialkylsilyl groups that are readily removed with F^- in protic solvents. We initially tested several trialkylsilyl groups, including the fluorine-containing ones, for monitoring their removal on the films by X-ray photoelectron spectroscopy (XPS). Unfortunately, the desilylation on these monolayers with F^- in various solvents was sluggish, requiring a high concentration of F^-, long reaction time, and high temperatures (data not shown).

In search for a protecting group for terminal alkynes that could be removed under very mild, neutral conditions, we turned our attention to the trimethylgermanyl (TMG) group.[39] Cai, Ernst, and Vasella found that the TMG group on terminal alkynes could be readily removed in protic solvents in the presence of catalytic amounts of Ag^+ or Cu^+.[39] The reaction probably starts by the formation of Ag^+ or Cu^+ complexes with the protected alkyne leading to a β-vinyl cation that is more stabilized by Ge than by Si through hyperconjugation (β-effect).[40] The subsequent degermylation followed by protonation of the metal acetylide intermediate provides the deprotected alkyne. In this work, the monolayers presenting C≡C−TMG groups (film **A**, Scheme 1) were prepared from the alkenyne **2** by photoactivated hydrosilylation on H-terminated silicon (111) surfaces.[21] The films were characterized by ellipsometry, contact angle, atomic force microscopy (AFM), and XPS. The ellipsometric thickness of the monolayer was 56 ± 1 Å, close to the estimated molecular length (59 Å). Selected XPS spectra of the TMG-terminated films **A** (Scheme 1) are presented in Figure 1a−d. The survey scan of the film **A** (Figure 1a) shows the presence of C, O, Ge, and Si. The narrow scan in the C1s region (Figure 1b) displays two deconvoluted signals at 286.7 and 285.0 eV, assigned to the etheric (**C**−O) and the rest of the carbon atoms, respectively. The ratio of areas derived from curve fitting was 1.36, similar to the stoichiometric ratio (1.38). A narrow scan of the Ge3d region (Figure 1c, empty circle) showed a strong emission at 31.4 eV, assigned to the TMG group. The ratio of C/O/Ge was found to be 1:0.30:0.029, similar to the stoichiometric value of 1:0.29:0.026. A narrow scan of the Si2p region (Figure 1d, empty circle) showed the absence of any emission at 101−104 eV regions; thus, no detectable oxide or suboxide silicon was present. The water contact angle of film **A** was 62° ± 1°, and remained similar (59° ± 1°) upon removal of the TMG group to form film **B**. In comparison, a higher water contact angle of ∼87° was reported for alkynyl-terminated monolayers.[31] The lower water contact angles for both films **A** and **B** may be due to the amorphous or liquid-like state of the OEG chains, as illustrated in Scheme 1 for film **A**, which allows

(38) Ng, A.; Ciampi, S.; James, M.; Harper, J. B.; Gooding, J. J. *Langmuir* **2009**, *25*, 13934–13941. Scheres, L.; Arafat, A.; Zuilhof, H. *Langmuir* **2007**, *23*, 8343–8346.

(39) Cai, C. Z.; Vasella, A. *Helv. Chim. Acta* **1995**, *78*, 732–757. Ernst, A.; Gobbi, L.; Vasella, A. *Tetrahedron Lett.* **1996**, *37*, 7959–7962.

(40) Dallaire, C.; Brook, M. A. *Organometallics* **1990**, *9*, 2873–2874. Eaborn, C.; Walton, D. R. M. *J. Organomet. Chem.* **1964**, *2*, 95–97.

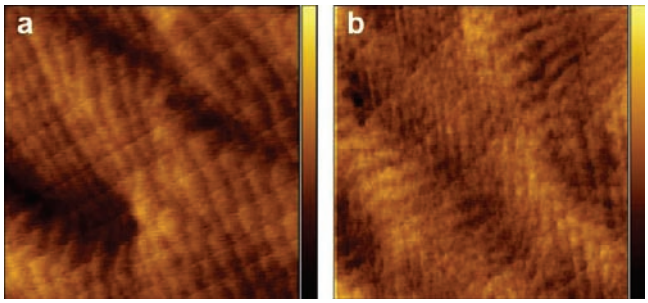

Figure 2. Tapping mode AFM images ($3 \times 3\ \mu m^2$) of the TMG−alkynyl-terminated film **A** before (a) and after (b) CuAAC reaction with the OEG-azide **4**. The *z* scale (contrast) for both images is 3 nm.

for a portion of the hydrophilic OEG chains to dynamically interact with water at the interface.

A typical atomic force microscopy (AFM) image of film **A** is shown in Figure 2a. Remarkably, the atomic steps of the silicon (111) substrate underneath the 56 Å thick film are clearly visible, indicating that the films were homogeneous. The corresponding root-mean-square (rms) roughness was 0.34 nm.

The deprotection of the alkynyl groups was monitored ex situ by the decrease of the Ge3d signal intensity (Figure 1c, solid dots). Indeed, the degermanylation was greatly promoted by Cu^+ in aqueous solution. At a copper concentration of 1.25 mM, it was completed within 30 min. Ascorbic acid served to reduce the air-oxidized copper to the catalytically active Cu^+. We found that Ag^+ was more efficient for the degermenylation but did not facilitate the subsequent CuAAC reaction. Remarkably, Cu^+ ligands that enhance the CuAAC reaction (see below) did not affect the degermanylation.

Direct CuAAC Reactions on the TMG−Alkynyl-Terminated Films. The main advantage of using the TMG protecting group is that its removal proceeds faster than the CuAAC reaction, both being promoted by Cu^+. Hence, they can be combined into one step for direct attachment of the azides **3**−**7** to films **A** (Scheme 1). Indeed, XPS data (Figure 1) supported that films **A** underwent CuAAC reaction with the CF_3-terminated azide **3** (5 mM) in the presence of $Cu(MeCN)_4PF_6$ (1.25 mM) and ascorbic acid (25.0 mM). The F1s signal appeared at 690 eV (Figure 1e) and N1s at 401 eV (Figure 1f), accompanied by the reduction of the Ge3d signal intensity by 95% (Figure 1c). The N1s signal was deconvoluted and fitted to three peaks assigned to CO**N**H (400.1 eV), N−**N**=**N** (400.8 eV), and **N**−N=N (401.7 eV), the ratio of the peak areas being about 1.2:2:1. The assignment of the N1s signals from the triazole ring is supported by the reported XPS data and density-functional theory calculation for some aromatic compounds containing sp^2 N atoms bonded to two or three atoms, showing that the N1s signal from the former is ∼1 eV lower than the latter.[41] No signal was present at ∼403 eV, corresponding to the central, electron-deficient N atom in the azido group, indicating no physisorption of **3** in the film.[42] The atomic concentration ratio N/F was 1.3, consistent with the value of 1.33 from the molecular formula. On the basis of the C/F and C/N ratios, the reaction yield was estimated to be ∼42% (Table 1). This value is similar to the yield (50%) derived from the increase of ellipsometric thickness (10 ± 2 Å) vs the calculated increase of molecular length (Table 1). Narrow scan of the Si2p region showed no detectable SiO*x* species in the 102−104 eV region (Figure 1d, solid dot).

Minimizing Oxidative Degradation of the Films. Although it was convenient that the azides could be directly grafted to the TMG−alkynyl surfaces **A**, the reaction time (12 h) was long and the yield (∼42%) was unsatisfactory. Similarly low efficiency was reported for CuAAC reactions on other alkynyl-presenting surfaces[30,31,44] and was attributed to steric hindrance.[30] During optimization of the reaction conditions, we found that O_2 substantially decreased the yields, likely due to the facile oxidation of Cu^+ to the catalytically inactive Cu^{2+} that may also promote the homocoupling of the adjacent alkynes.[45] Furthermore, the redox cycle of Cu^+/Cu^{2+} in the presence of O_2 and sodium ascorbate generates oxy radicals[26] that may degrade the OEG film.[19] Hence, we performed the reactions in a N_2 environment. Next, we tested a series of copper concentrations in the range of 0.3−10 mM. When the copper concentration was below 1 mM, the reaction was sluggish. Notably, the yields were not affected by the copper concentrations in the range of 2.5−10 mM. After the reaction, the harmful copper residue could be removed by washing with an EDTA solution, as confirmed by the absence of the $Cu2p_{3/2}$ signal near 933 eV.

Improved Copper Catalyst. Recently, several series of Cu^+ ligands have been investigated to accelerate CuAAC reactions.[25,46,47] Among them, the commercially available tris-triazole **8**[46] (TBTA, Scheme 1) has been most widely used. Unfortunately, we found that this ligand was ineffective for promoting surface CuAAC reactions in our systems, probably due to the steric hindrance of the ligand and the surface alkyne groups. We then tested several smaller ligands similar to the monotriazole **9** reported by Fokin and co-workers[46] and identified the most efficient ligand **10**. The OEG chain in **10** renders the Cu^+ complex water soluble, and the electron-donating $NHCH_3$ group maintains a high catalytic activity of the complex. Indeed, grafting of the CF_3-terminated azide **3** onto the TMG−ethynyl-terminated films **A** was greatly accelerated by the ligand **10**, as shown by Figure 3 plotting the increase of the atomic concentration ratio F/C of the film over time in the presence and absence of the ligand **10**. In the presence of **10**, the reaction was completed in ∼2 h as compared to 12 h without the ligand. The yield (65−76%) of the optimized reaction leading to film **C** was estimated by the F/C and N/C ratio and the increase of the ellipsometric thickness (Table 1). The yield derived from the F/C ratio is higher, likely due to the ignorance of the attenuation factor, leading to an overestimate of the F/C ratio, especially for the dense OEG top layer where the CF_3 terminal groups are populated closer to the film surface.

Preparation of Films D−F. Using the above optimized conditions, the azides **4**−**6** were attached onto the TMG-terminated films **A** to provide the films presenting OEG (**D**),

(41) Ito, E.; Oji, H.; Araki, T.; Oichi, K.; Ishii, H.; Ouchi, Y.; Ohta, T.; Kosugi, N.; Maruyama, Y.; Naito, T.; Inabe, T.; Seki, K. *J. Am. Chem. Soc.* **1997**, *119*, 6336–6344. Alfredsson, Y.; Brena, B.; Nilson, K.; Ahlund, J.; Kjeldgaard, L.; Nyberg, M.; Luo, Y.; Martensson, N.; Sandell, A.; Puglia, C.; Siegbahn, H. *J. Chem. Phys.* **2005**, *122*, 6.
(42) Collman, J. P.; Devaraj, N. K.; Eberspacher, T. P. A.; Chidsey, C. E. D. *Langmuir* **2006**, *22*, 2457–2464.
(43) Petrovykh, D. Y.; Kimura-Suda, H.; Tarlov, M. J.; Whitman, L. J. *Langmuir* **2004**, *20*, 429–440.
(44) Lin, P. C.; Ueng, S. H.; Yu, S. C.; Jan, M. D.; Adak, A. K.; Yu, C. C.; Lin, C. C. *Org. Lett.* **2007**, *9*, 2131–2134.
(45) Eglinton, G.; McCrae, W. *Adv. Org. Chem.* **1963**, *4*, 225.
(46) Chan, T. R.; Hilgraf, R.; Sharpless, K. B.; Fokin, V. V. *Org. Lett.* **2004**, *6*, 2853–2855.
(47) Rodionov, V. O.; Presolski, S. I.; Gardinier, S.; Lim, Y. H.; Finn, M. G. *J. Am. Chem. Soc.* **2007**, *129*, 12696–12704. Rodionov, V. O.; Presolski, S. I.; Diaz, D. D.; Fokin, V. V.; Finn, M. G. *J. Am. Chem. Soc.* **2007**, *129*, 12705–12712.

Table 1. XPS and Ellipsometry Derived Yields for the Grafting of the Azides **3**−**6** under CuAAC Reaction Conditions[a,b] onto the TMG−Alkynyl Films **A** To Form Films **C**−**F**

	XPS				ellipsometry		
films	C/F ratio	yield[c] (%)	C/N ratio	yield[d,e] (%)	Δd_{exp}[f] (Å)	Δd_{calc}[g] (Å)	yield[h] (%)
C[a]	32 ± 6	43	25 ± 5	41[d]	10 ± 2	20	50
C[b]	20 ± 4	76	17 ± 3	65[d]	13 ± 2	20	65
D[b]			19 ± 4	75[e]	10 ± 2	14	71
E[b]			22 ± 4	72[e]	13 ± 2	21	62
F[b]			22 ± 4	72[e]	12 ± 2	21	57

[a] Azide **3** (5 mM), $Cu(MeCN)_4PF_6$ (1.25 mM), and ascorbic acid (25 mM) in EtOH/H_2O 1:1, 25 °C in air, 12 h. [b] Azide (5 mM, **3** for **C**, **4** for **D**, **5** for **E**, **6** for **F**), $Cu(MeCN)_4PF_6$ (1.25 mM), the ligand **10** (12.5 mM), and ascorbic acid (25 mM) in EtOH/H_2O 1:1, 25 °C in nitrogen, 4 h. [c] Yield (x%) is derived from C/F = (35 + 14x%)/3x%, where C/F is the atomic ratio measured by XPS with a random uncertainty of ∼20%,[43] 3 is the number of F atoms in the azide **3**, and 35 and 14 are the number of C atoms in the alkyne (after degermenylation of **2**) and the azide **3**, respectively. [d] Yield (x%) is derived from C/N = (35 + 14x%)/4x%, where C/N is the atomic ratio measured by XPS with a random uncertainty of ∼20%,[43] 4 is the number of N atoms in the azide **3**, and 35 and 14 are the number of C atoms in the degermenyled alkyne and the azide **3**, respectively. [e] Yield (x%) is derived from C/N = (35 + N_C x%)/3x%, where C/N is the atomic ratio measured by XPS with a random uncertainty of ∼20%,[43] 3 is the number of N atoms in the azides **4**−**6**, 35 is the number of C atoms in the degermenyled alkyne, N_C is the number of C atoms in the corresponding azide (10 for **4** and 18 for **5** and **6**). [f] Δd_{exp} is the difference of the film thickness measured by ellipsometry before and after grafting of the corresponding azides **3**−**6** to the film **A**. The standard deviations of the thickness measurement were within ±1 Å, leading to an uncertainty of ±2 Å for Δd_{exp}. [g] Δd_{calc} is the calculated increase of the molecular length of the TMG−alkyne **2** after CuAAC reaction with the corresponding azides. The molecular length increased from 59 Å for **2** to 79 Å after coupling with **3**, 73 Å with **4**, and 80 Å with **5** and **6**. [h] Yield (%) = $\Delta d_{exp}/\Delta d_{calc}$.

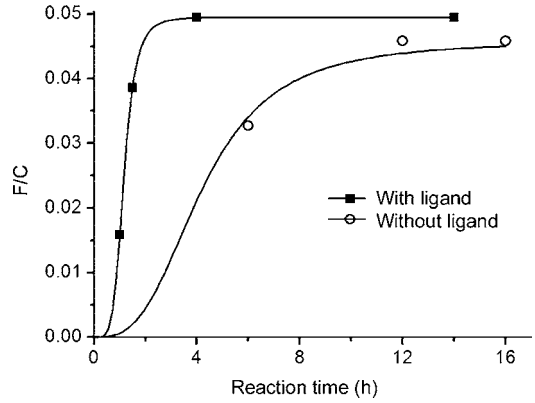

Figure 3. Progress of the CuAAC reaction on the TMG−alkynyl-terminated films **A** with the CF_3-terminated azide **3**, monitored ex situ by the F/C ratio of the film after various reaction times in the presence (square) and absence (circle) of the ligand **10** under otherwise identical conditions: $Cu(MeCN)_4PF_6$ (1.25 mM), ascorbic acid (25 mM), the azide **3** (5 mM), and the ligand **10** (12.5 mM) in EtOH/H_2O 1:1 at 25 °C. Each data point was obtained by reacting a film **A** in the reaction mixture for the given time, followed by cleaning and measuring of the F/C ratio of the film by XPS. The curve serves to guide the eyes.

mannose (**E**), and glucose (**F**) (Scheme 1). The yields of the reactions were estimated from the XPS C/N ratio and the increase of the ellipsometric thickness. As shown in Table 1, the yields derived by both methods were consistent within the ∼20% random uncertainty[43] for XPS measurement of the N1s signals and the ±2 Å uncertainty for measurement of the increase of thickness. The yield (71−75%) for grafting the OEG−azide **4** was a substantial improvement over the reported ones on other systems.[30] Most importantly, the resultant OEG-presented surfaces **D** were highly protein resistant (see below). The slightly lower efficiency for grafting the sugars **5** and **6** is probably due to the steric hindrance of the sugar.

Films Presenting OEG (D). Upon the CuAAC reaction leading to film **D**, the ellipsometric thickness increased to 68 ± 1 Å, similar to the calculated molecular length of 73 Å, indicating a high density of the OEG chains grafted onto the film **A**, although determination of the exact OEG density on such thick films is beyond the scope of this work. The homogeneity of the films was maintained after the reaction, as indicated by the AFM image (Figure 2b), showing the atomic steps of the underlying silicon substrate, and by the small rms roughness of 0.35 nm. XPS data show the disappearance of the Ge3d signal (Figure 4a) and the appearance of the N1s signal (Figure 4b) that can be deconvoluted into two peaks at binding energies of 400.1 and 401.1 eV with an intensity ratio of 2:1, corresponding to the triazole moieties. The C1s signal is deconvoluted into two peaks at 286.3 eV for **C**−O and **C**−N and at 284.8 eV for the alkyl carbon atoms.

Protein Resistance of Films D. The protein resistance of the above OEG-modified films **D** was evaluated by XPS measurement of the amount of adsorbed fibrinogen after incubation in a 0.1% fibrinogen solution in PBS for 1 h, followed by gentle washing with Millipore water for only ∼30 s. The increase of the N1s signal intensity relative to that of a standard monolayer of fibrinogen[17] indicated that only about (1.6 ± 0.8)% (n = 4) monolayer of the protein was adsorbed on the OEG-modified film **D**. Note that fibrinogen possesses ∼4300 nitrogen atoms, leading to a detection limit of ∼0.8% monolayer. Indeed, the N1s signals before and after treatment with the fibrinogen solution almost completely overlap each other (Figure 4c, the squares and dots behind the squares). Factors influencing the protein resistance of OEG monolayers are still not well understood.[48] The high protein resistance of film **D** may be associated with the appropriate density of the OEG chains and their amorphous/liquid-like state, as illustrated in Scheme 1, which promotes tight binding of water.[48]

Films Presenting Mannose (E) and Glucose (F). Upon grafting the mannose−azides **5** onto the TMG-terminated films **A**, the ellipsometric thickness of the film increased to 71 ± 1 Å, not much behind the calculated molecular length of ∼80 Å. The yield of the reaction was estimated to be 62−72% (Table 1). Considering the relatively large size of the mannose moiety, the grafting is quite efficient. The water contact angle on the resultant film **E** decreased from 62° ± 1° to 33° ± 2°. XPS narrow scan for C1s of films **E** show the increase of the etheric C1s signal at 286.3 eV. The N1s signal (Figure 4f) can be deconvoluted into two peaks at binding energies of 400.0 eV for **N**−N═N and 401.1 eV for N−**N**═**N** with an intensity ratio of 1:2. Unreacted mannose−azides were not present after the CuAAC reaction, as no apparent peak was observed near 403

(48) He, Y.; Chang, Y.; Hower, J. C.; Zheng, J.; Chen, S. F.; Jiang, S. *Phys. Chem. Chem. Phys.* **2008**, *10*, 5539–5544. Zolk, M.; Eisert, F.; Pipper, J.; Herrwerth, S.; Eck, W.; Buck, M.; Grunze, M. *Langmuir* **2000**, *16*, 5849–5852.

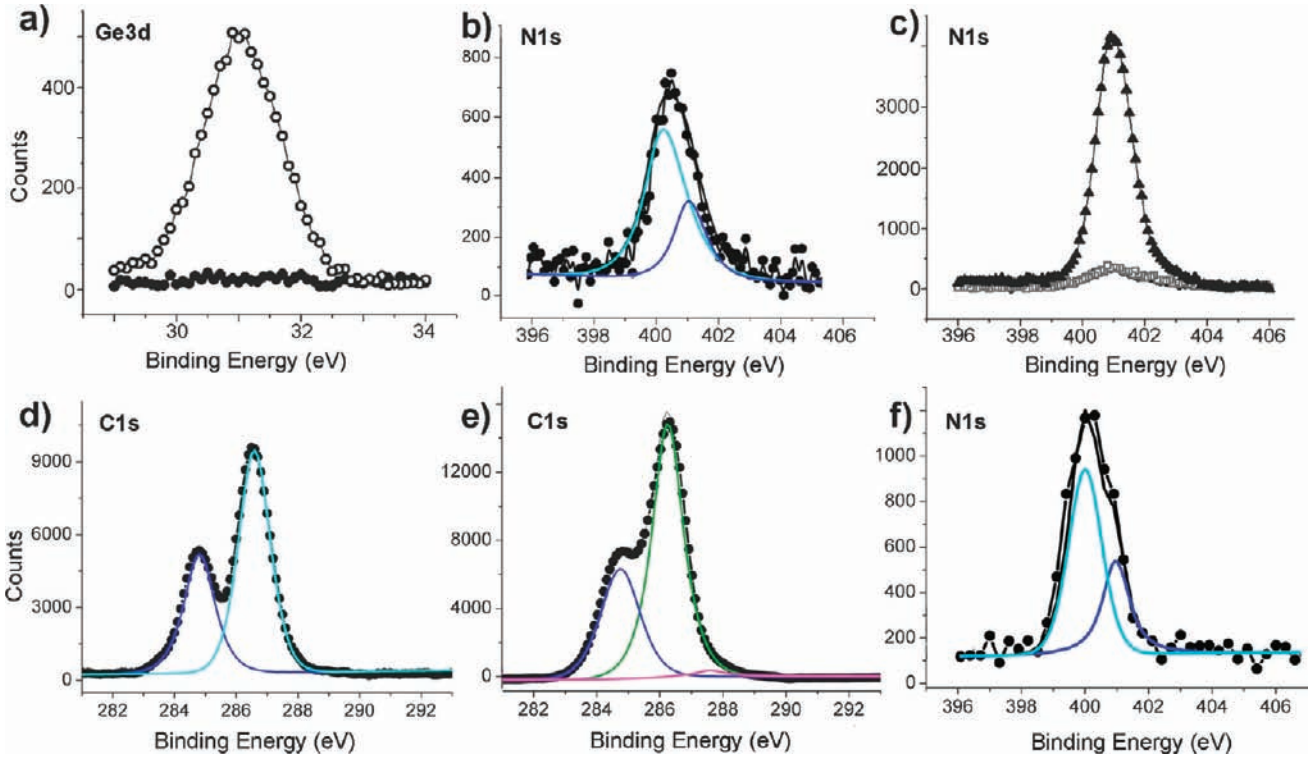

Figure 4. Selected XPS narrow scans for Ge3d, N1s, and C1s of films **D** and **E** prepared from **A** via CuAAC reaction with the azides **4** and **5** (Scheme 1), respectively. The data for films **D** include Ge3d (a, solid dots for film **D** vs empty circles for film **A** before the reaction), N1s (b, with deconvolution), N1s before (c, dots behind the squares) and after (c, squares) treatment with a 0.1% fibrinogen solution vs the N1s signal of a monolayer of fibrinogen (triangle) adsorbed on a H−Si (111) surface, and C1s (d, with deconvolution). The data for films **E** include the deconvoluted C1s (e) and N1s (f) signals.

eV. The thickness, contact angle, and XPS data for the glucose-presenting films **F** were similar to those of the mannose-presenting films **E**.

Specific Adherence of Bacteria to Mannose-Presenting Surfaces (E). To demonstrate that the thin film platforms can be functionalized via CuAAC reaction to capture specific living biological targets, we used the mannose-modified film **E** to interact with *E. coli* 83972 strains with or without mannose-binding type-1 fimbrae (*fim*+ or *fim*-). Previously, self-assembled alkanethiol monolayers presenting mannose on gold substrate surfaces were used to capture *E. coli* expressing fimbrae,[49] albeit without comparison with the bacteria that do not possess fimbrae. The mannose-presenting films **E** were incubated overnight in Luria−Bertani media containing either *fim*+ or *fim*- *E. coli* 83972. As controls, films presenting either glucose (**F**) or ethynyl groups (upon degermanylation of **A**) were likewise exposed to these organisms under identical conditions. As shown by Figure 5a and 5f, the *fim*+ *E. coli* nearly fully covered the mannose-presenting surfaces while the *fim*- strain did not adhere to the surfaces (Figure 5b and 5f). In addition, very few *fim*+ *E. coli* attached on the glucose-presenting surface (Figure 5c and 5f). Furthermore, no *fim*+ *E. coli* were seen on the OEG−alkynyl-terminated surface **B** (Figure 5d and 5f). Finally, preincubation of the *fim*+ *E. coli* strain with mannose substantially reduced their subsequent adherence to the mannose-presenting surface (Figure 5e and 5f). These results clearly demonstrate that the binding of *fim*+ *E. coli* is specifically between the mannose binding receptors on the bacterial fimbrae and the mannose presented on the surface **E**. The reason for the ability of OEG−alkynyl-presenting film **B** to repel *fim*+ *E. coli* is unclear. Understanding the factors influencing bacterial adhesion to surfaces is in its infancy.[50] In general, modification of surfaces with OEG and PEG reduces bacterial adhesion to various extents depending on the bacterial species.[51]

Attachment of Biotin and Mannose in Microarray Format. The versatility of the TMG−alkynyl-terminated monolayers **A** was demonstrated by performing the multicomponent CuAAC reactions in microarray format (Scheme 2). Biotin and mannose with an azido handle (compounds **7** and **5**) were mixed with the OEG azide **4** at ratios of 1:0, 1:1, and 1:9, together with other reagents at a ratio of azide/$CuSO_4$/ligand **10**/ascorbic acid 1:1.6:11:19, and were then spotted on the film. The spotting of the mixture of reagents and the subsequent reactions on the surface were performed in an anaerobic chamber under N_2 atmosphere with a relative humidity of 60% for 4 h. The remaining surface was then backfilled with OEG via CuAAC reaction with the OEG-N_3 **4** to resist nonspecific adsorption of

(49) Qian, X. P.; Metallo, S. J.; Choi, I. S.; Wu, H. K.; Liang, M. N.; Whitesides, G. M. *Anal. Chem.* **2002**, *74*, 1805–1810. Barth, K. A.; Coullerez, G.; Nilsson, L. M.; Castelli, R.; Seeberger, P. H.; Vogel, V.; Textor, M. *Adv. Funct. Mater.* **2008**, *18*, 1459–1469. Pieters, R. J. *Med. Res. Rev.* **2007**, *27*, 796–816. Rozhok, S.; Shen, C. K. F.; Littler, P. L. H.; Fan, Z. F.; Liu, C.; Mirkin, C. A.; Holz, R. C. *Small* **2005**, *1*, 445–451.

(50) Burton, E. A.; Sirnon, K. A.; Hou, S. Y.; Ren, D. C.; Luk, Y. Y. *Langmuir* **2009**, *25*, 1547–1553. Cheng, G.; Li, G. Z.; Xue, H.; Chen, S. F.; Bryers, J. D.; Jiang, S. Y. *Biomaterials* **2009**, *30*, 5234–5240.

(51) Harris, L. G.; Tosatti, S.; Wieland, M.; Textor, M.; Richards, R. G. *Biomaterials* **2004**, *25*, 4135–4148. Roosjen, A.; Busscher, H. J.; Nordel, W.; van der Mei, H. C. *Microbiology (UK)* **2006**, *152*, 2673–2682. Chapman, R. G.; Ostuni, E.; Liang, M. N.; Meluleni, G.; Kim, E.; Yan, L.; Pier, G.; Warren, H. S.; Whitesides, G. M. *Langmuir* **2001**, *17*, 1225–1233. Kingshott, P.; Wei, J.; Bagge-Ravn, D.; Gadegaard, N.; Gram, L. *Langmuir* **2003**, *19*, 6912–6921. Ostuni, E.; Chapman, R. G.; Liang, M. N.; Meluleni, G.; Pier, G.; Ingber, D. E.; Whitesides, G. M. *Langmuir* **2001**, *17*, 6336–6343.

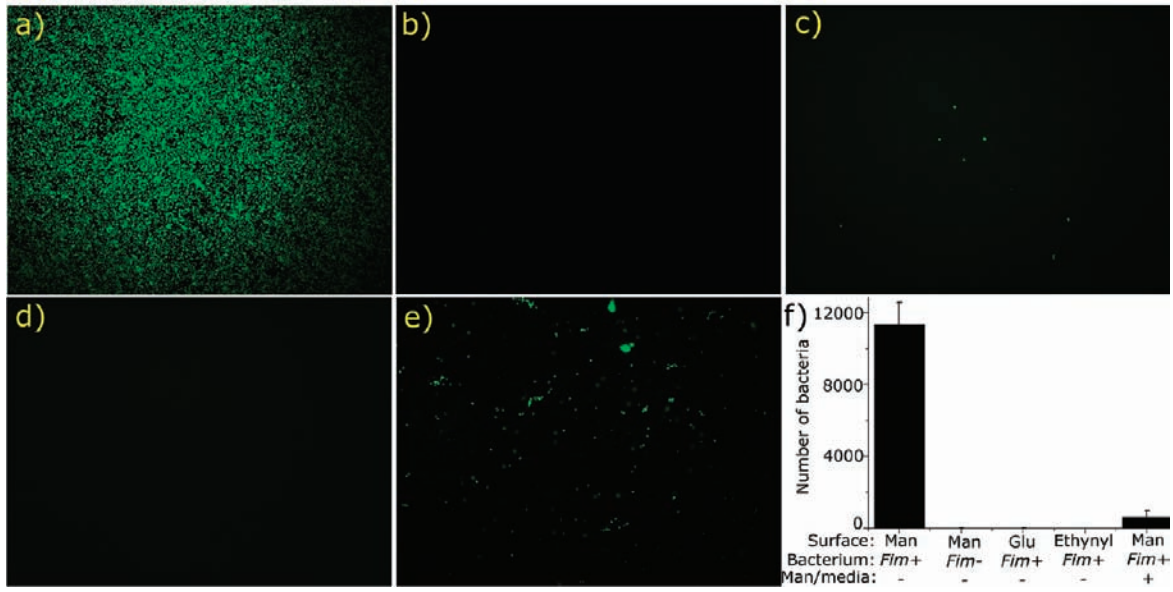

Figure 5. Fluorescent images (a−e) of various modified surfaces incubated with *fim*+ and *fim*- *E. coli*, and a plot (f) of the numbers of *E. coli* in all images with a standard deviation on these surfaces. The combinations depicted are the mannose-presenting film **E** and *fim*+ *E. coli* (a, bacterial count 11 313 ± 1241 for f), film **E** and *fim*- *E. coli* (b, bacterial count 1 ± 1 for f), the glucose-presenting films **F** and *fim*+ *E. coli* (c, bacterial count 7 ± 1 for f), the ethynyl-presenting films **B** and *fim*+ *E. coli* (d, bacterial count: 0 ± 0 for f), and film **E** and the *fim*+ *E. coli* that had been presaturated with mannose in the media (e, bacterial count 627 ± 352 for f). Each image is representative of up to 20 images obtained on random locations at the sample surface (for examples, see Figures S2−S6 in the Supporting Information).

Scheme 2. Attachment of the Biotin-N_3 **7** and Mannose-N_3 **5** with the OEG-N_3 **4** on the TMG−Alkynyl-Terminated Films **A** via CuAAC Reaction, Followed by Backfilling with the OEG-N_3 **4** and Binding with FITC-Labeled Avidin and Con A

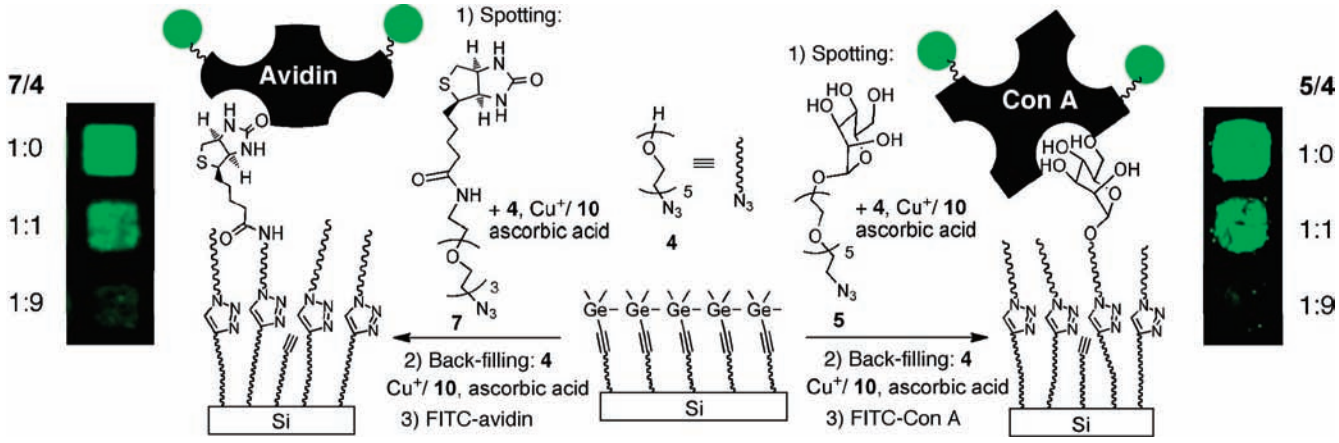

proteins. The samples were then incubated in solutions of avidin and Concanavalin A (Con A), both labeled with fluorescein isothiocyanate (FITC). Selective binding of the proteins to the ligands immobilized via CuAAC reaction is shown in the fluorescent images (Scheme 2). The amount of bound proteins decreases with the ratio of the biotin azide **7** or the mannose azide **5** relative to the OEG azide **4**. The control experiment with avidin-FITC saturated with biotin or FITC-ConA saturated with mannose showed no binding to the biotin- or mannose-presenting spots, thus establishing that the bindings were specific.

Conclusion

We developed a versatile monolayer platform presenting trimethylgermanyl (TMG)-protected alkynyl groups on silicon substrates that allows for direct tethering of biomolecules via CuAAC reaction in good yields. Significantly, the efficient grafting of OEG chains onto this platform provided an OEG-terminated surface that is highly resistant to nonspecific adsorption of proteins, thus addressing the key issue of nonspecific binding on the functionalized monolayers on nonoxidized silicon. Moreover, the CuAAC reaction mixtures can be spotted on the platform and the rest of the surface subsequently be passivated with OEG−azide to provide arrays/patterns of biomolecules with controlled composition on an inert background. We have also shown that upon attaching a mannose−azide to the monolayer platform, the resultant mannose-presenting surfaces can specifically capture *E. coli* expressing mannose-binding fimbriae. Furthermore, organogermanium has a low toxicity (it has been used in dietary supplements).[56] We expect that this "clickable" platform can be applied for biofunctionalization of a wide range of silicon-based materials, including porous membrane, nanoparticles, and nanowires.

Experimental Section

Materials. Sulfuric acid, 30% hydrogen peroxide solution, 40% ammonium fluoride solution, dichloromethane, *N*,*N*,*N*′,*N*′-tetramethylethane-1,2-diamine (EDTA), ascorbic acid, sodium ascorbate, $Cu(MeCN)_4PF_6$, $CuSO_4$, fluoresceine isothiocyanate (FTIC)-avidin,

fibrinogen, and FTIC-Con A were purchased from Sigma-Aldrich, silicon (111) wafers from Silicon Quest International. Inc., and absolute ethanol from Alfa Aesar. The syntheses of compounds **2**−**7** are provided in the Supporting Information.

Ellipsometry. Thickness measurements were performed on a Multiskop system (Optrel GmbH, Germany) or an Auto EL III ellipsometer (Rudolph Research) equipped with a 632.8 nm He−Ne laser source at an incident angle of 60° or 70°. The optical constants of the substrate were determined with a piece of freshly prepared H−Si(111) wafer ($n = 3.839$ and $k = 0.016$). The thicknesses of the monolayers were determined with assumed refractive indices of 1.45 for the organic monolayer. At least three measurements in random locations were taken for each sample, and the mean values were reproducible within ±1 Å.

Estimation of Molecular Length. The molecular length was estimated by molecular mechanics modeling with MM2 in Chem3D Ultra 10.0 (CambridgeSoft).

Contact Angle Goniometry. Contact angles were measured on a Rame-Hart model 100 goniometer under ambient conditions. Both edges of 3 drops of the contacting liquids (water) were measured on random locations of the surface for each sample.

X-ray Photoelectron Spectroscopy (XPS). XPS was performed with a PHI 5700 X-ray photoelectron spectrometer equipped with a monochromatic Al Kα X-ray source (1486.7 eV) at a takeoff angle (TOA) of 45° from the film surface. The spectrometer was operated at both high and low resolutions with window pass energies of 23.5 and 187.85 eV, respectively. Electron binding energies were calibrated with respect to the C1s line at 286.4 eV (C−C) or the Si2p line at 99.0 eV. The atomic concentrations were estimated by the PHI Multipak 5.0 software (Physical Electronics) using the standard procedure including the Shirley background subtraction and corrections with the corresponding Scofield atomic sensitivity factors, assuming a homogeneous distribution of the atoms to a depth of a few nanometers. Signal deconvolution was performed first by Shirley background subtraction, followed by nonlinear fitting to mixed Gaussian−Lorentzian functions with 80% Gaussian and 20% Lorentzian character.

Atomic Force Microscopy (AFM). AFM imaging of the surfaces was performed using a MultiMode Nanoscope IIIa AFM (Digital Instruments Inc., Santa Barbara, CA). Images were acquired in tapping mode using a silicon nitride cantilever (MikroMasch, San Jose, CA) with a resonance frequency of 132.9 kHz and a nominal force constant of 1.75 N/m.

Fluorescence Microscopy. Fluorescent images were obtained with an Olympus BX 51 fluorescence microscope. Images were processed using QCapture software (QImaging Co.).

Preparation of H−Si(111) Substrates. Single-side polished, p-type (boron-doped, 1−10 Ω·cm resistivity) silicon (111) wafers (Silicon Quest International, Inc.) were cut into pieces of 2 × 2 cm^2 and cleaned with Piranha solution (concentrated H_2SO_4/30% H_2O_2 3:1 v/v) for 20−30 min at ∼80 °C to remove organic contaminates. *Caution: Piranha solutions react violently with organic materials and should be handled with extreme care.* The freshly cleaned sample was immersed in an argon-saturated, 40% NH_4F solution for 20 min followed by rapid rinse with argon-saturated Millipore water and dried with a stream of nitrogen.

Monolayers Terminated with TMG−C═C Groups. The apparatus and procedure for surface hydrosilylation was described elsewhere.[20] Briefly, a freshly prepared H−Si(111) substrate was placed on top of a *z* translational manipulator inside a homemade vacuum chamber. After degassing for 10 min at 10^{-4} Torr, the sample was brought in contact with a droplet (ca. 2−3 mg) of the alkene **2** on a quartz window, forming a uniform layer of the alkene sandwiched by the quartz window and the silicon substrate. Hydrosilylation was performed under 254 nm UV illumination with a handheld illuminator (Spectroline Co.) for 2 h. The sample was washed thoroughly with dichloromethane and absolute ethanol followed by drying under a stream of argon.

Removal of the TMG Protecting Groups. Under N_2 environment, the above monolayers presenting TMG−alkynyl groups were immersed in a solution of $CuSO_4$ (1.25 mM), sodium ascorbate (25 mM), and the ligand **10** (12.5 mM) in degassed water or a solution of $Cu(MeCN)_4PF_6$ (1.25 mM) or $AgNO_3$ (1.25 mM), ascorbic acid (25 mM), and the ligand **10** (12.5 mM) in degassed MeOH/EtOH/H_2O (2:1:1) for 10−60 min, followed by washing with Millipore water and immersion in 25 mM EDTA solution, sonication in EtOH/MeOH (1:1) for 30 s and then in Millipore water for 30 s, and drying with a stream of nitrogen.

Surface CuAAC Reactions. Under nitrogen, a TMG-terminated substrate **A** was immersed in a solution of $Cu(MeCN)_4PF_6$ (1.25 mM), an azide (5 mM), the copper ligand **10** (12.5 mM), and ascorbic acid (25 mM) in degassed methanol/water (1:1 v/v). Alternatively, the reaction could be performed in a solution of $CuSO_4$ (1.25 mM), an azide (5 mM), the copper ligand **10** (12.5 mM), and sodium ascorbate (25 mM) in degassed water. Both conditions gave similar results. After incubation for 4 h, the sample was taken out and immersed in 25 mM EDTA solution, sonicated for 10 s, thoroughly washed with Millipore water and then ethanol, and dried under a stream of argon.

Protein Resistance. XPS N1s signal intensity on an OEG-terminated film **D** (Scheme 1) was first measured. Immediately after the measurement, this sample and a freshly prepared hydrogen-terminated silicon (111) substrate were individually incubated in a fibrinogen solution (1 mg/mL in 0.01 M PBS buffer (pH 7.4), prepared without excessive shaking to avoid formation of long-lasting bubbles and possible denaturing of the protein) for 1 h. The sample was taken out and immediately washed with Millipore water for ∼30 s and dried with a flow of argon. The ellipsometric thickness of the protein film on the H−Si(111) surface was 61 ± 2 Å, corresponding to a monolayer of the protein.[17] Both dried films were immediately subjected to measurement of the N1s signal intensity. The protein resistance of film **D** is calculated by the increase of the N1s signal intensity after protein adsorption divided by the N1s signal intensity of the protein monolayer, and the data were obtained from four experiments.

Surface CuAAC Reactions in Microarray Format. Solutions of a mixture of azides (the biotin azide **7** or the mannose azide **5** mixed with the OEG azide **4** at a molar ratio of **5**/**4** or **7**/**4** = 1:0, 1:1, and 1:9 and total concentration of 3.33 mM), $CuSO_4$ (5.33 mM), the copper ligand **10** (37.0 mM), and sodium ascorbate (63.6 mM) in a 10:1 (v/v) mixed solution of PBS buffer and Micro Spotting Solution Plus 2x (TeleChem International, Inc., Sunnyvale, CA) were spotted on a TMG-terminated surface **A** using a Spotbot 2 Personal Microarray Robot (TeleChem International, Inc.) with a microarray spotting pin (946MP16). The spotter was placed in an anaerobic chamber filled with nitrogen, and the relative humidity in the chamber of the spotter was 60%. After spotting, the sample was allowed to incubate for 4 h in the chamber. The 10 nL droplets did not dry out during this period due to the presence of the above spotting solution that decreases evaporation. The samples were then rapidly washed with 10 mM EDTA solution (6 mL), PBS buffer (6 mL), and water and immediately immersed in a solution of the OEG-N_3 **4** (3.33 mM), $CuSO_4$ (5.33 mM), the copper ligand **10** (37.0 mM), and ascorbic acid (63.6 mM) in PBS buffer. The sample was allowed to incubate under N_2 for 4 h and then immersed in 10 mM EDTA for 10 min, followed by washing with water (6 mL) and drying in a stream of N_2.

Binding of Targeted Molecules. The above microarray samples were immersed in a solution of FITC-avidin (0.5 mg/mL) or FITC-Con A (0.5 mg/mL) in PBS buffer for 30 min in a humidified chamber. The sample was washed with water and dried immediately with a stream of argon. Fluorescent images of the microarrays were acquired using a GeneTAC UC-4 Array Scanner (Genomic Solutions) with a 488 nm excitation and 512 nm emission bandpass filter.

Specific Bacterial Adherence on Mannose-Modified Surfaces. Derivative strains of *E. coli* 83972[52] expressing type 1 fimbriae (*fim*+) or without type 1 fimbriae (*fim*-) were used in this study. *E. coli* 83972 is a nonpathogenic strain[52] that has been studied in vivo as a means to prevent catheter-associated urinary tract infection.[53,54] To create *fim*+ *E. coli* 83972 that binds to mannose, we transformed the wild-type *E. coli* 83972 with pSH2 encoding type 1 fimbriae[55] and pGreen encoding green fluorescent protein (GFP). We previously confirmed overexpression of type 1 fimbriae by this strain.[54] To create *fim*- *E. coli* 83972 that does not bind to mannose but has the same fluorescence and antibiotic resistance profile as *fim*+ *E. coli* 83972, we transformed wild-type *E. coli* 83972 with the empty pACYC vector and pGreen.

The ability of the derivative strains of *E. coli* 83972 to adhere to variously modified silicon substrates was assessed by the following assay. A silicon sample was placed in a 5 mL solution of 20 μg/mL chloramphenicol and 100 μg/mL ampicillin in Luria−Bertani (LB) broth (Difco Laboratories, MD). The broth was inoculated with a single colony of the given strain of bacteria from an agar plate and incubated with rocking at 37 °C overnight. The sample was rinsed 3 times in water prior to fluorescent imaging. Images of up to 20 randomly chosen visual fields were obtained for each sample. To confirm that the adherence of the bacteria was due to specific mannose-receptor binding, the *fim*+ *E. coli* 83972 was preincubated in the LB broth containing 50 mM mannose for 1 h (to saturate the mannose binding sites) prior to addition of a mannose-presenting substrate.

Acknowledgment. This work was supported by The Welch Foundation (E-1498), the NSF CAREER Award (CTS-0349228 to C.C.), and grant DMR-0706627, NIH R21 HD058985, NIH R21EY018303, Alliance for Nanohealth W81XWH-09-2-0139, and the Texas Center for Superconductivity at the University of Houston. The *E. coli* strain creation and adherence testing was supported by grants VA CDA-2 RR&D B4623 and NIH R21 DK077313.

Supporting Information Available: Synthesis of **2**−**7**, AFM image of H−Si(111) sample surface, and fluorescence images of various modified surfaces incubated with *fim*+ and *fim*- *E. coli*. This material is available free of charge via the Internet at http://pubs.acs.org.

JA1025497

(52) Andersson, P.; Engberg, I.; Lidinjanson, G.; Lincoln, K.; Hull, R.; Hull, S.; Svanborg, C. *Infect. Immun.* **1991**, *59*, 2915–2921.
(53) Sunden, F.; Hakansson, L.; Ljunggren, E.; Wullt, B. *Int. J. Antimicrob. Agents* **2006**, *28*, S26–S29. Trautner, B. W.; Hull, R. A.; Thornby, J. I.; Darouiche, R. O. *Infect. Control Hosp. Epidemiol.* **2007**, *28*, 92–94.
(54) Trautner, B. W.; Cevallos, M. E.; Li, H. G.; Riosa, S.; Hull, R. A.; Hull, S. I.; Tweardy, D. J.; Darouiche, R. O. *J. Infect. Dis.* **2008**, *198*, 899–906.
(55) Hull, R. A.; Gill, R. E.; Hsu, P.; Minshew, B. H.; Falkow, S. *Infect. Immun.* **1981**, *33*, 933–938.
(56) Tao, S.-H.; Bolger, P. M. *Regul. Toxicol. Pharmacol.* **1997**, *25*, 211–219.